Inorg. Chem. **2006**, *45*, 7962–7967

Distinct Water-Exchange Mechanisms for Trinuclear Transition-Metal Clusters

Jacqueline R. Houston,[†] David T. Richens,[‡] and William H. Casey*[,†,§]

Departments of Chemistry and Geology, University of California, Davis, California 95616, and Chemistry Department, University of St. Andrews, North Haugh, St. Andrews, KY16 9ST, Scotland, United Kingdom

Received May 31, 2006

Mechanisms for water exchange from the bioxo-capped M–M-bonded trinuclear clusters, $[M_3(\mu_3\text{-}O)_2(\mu\text{-}O_2CCH_3)_6(OH_2)_3]^{2+}$ [M = Mo(IV) and W(IV)], were investigated using high-pressure ^{17}O NMR and compared to our previous work on a similar Rh(III) trimer. Reaction rates decrease by more than a factor of 2 when pressure is increased from 6 to 250 MPa for the Mo(IV) trimer, while exchange rates increase by less than a factor of 1.2 (10–229 MPa) for the W(IV) trimer. From the pressure dependence of the reaction rate, activation volumes ($\Delta V^{\ddagger}$) were calculated to be $\Delta V^{\ddagger} = +8.0$ (± 0.4) cm^3 mol^{-1} and $\Delta V^{\ddagger} = -1.9$ (± 0.2) cm^3 mol^{-1} for the Mo(IV) cluster and W(IV) cluster, respectively, which is the largest difference ($\sim$10 cm^3 mol^{-1}) in activation volumes for any pair of 4d–5d (and 3d–4d) transition metal species located within the same group of the periodic table. If we interpret these activation volumes in terms of Swaddle's semiempirical model, which he established for simple octahedral monomers (Associative (A) = $\Delta V^{\ddagger} \approx -13$; Interchange (I) = $\Delta V^{\ddagger} \approx 0$; or Dissociative (D) = $\Delta V^{\ddagger} \approx +13$), our results suggest that water exchange follows a dissociative–interchange (I_d) mechanism for the Mo(IV) cluster and an associative–interchange (I_a) activation mode for the W(IV) trimer. These volumes exhibit a unique changeover in the water-exchange mechanism despite considerable similarities in molecular structure and reactivity. This changeover could provide a standard for computational simulations of ligand-exchange pathways in molecules that are more complicated than monomers.

Introduction

Activation volumes calculated from high-pressure NMR measurements have been used for nearly three decades to assign mechanisms for ligand-exchange reactions.[1] Merbach et al.[2−8] and Swaddle[4,9−13] were pioneers in this field and demonstrated that activation pathways for water-exchange mechanisms become increasingly associative (A) for aqueous metal ions as one moves down the same group of the periodic table [e.g., $[Fe(OH_2)_6]^{2+}$ (+3.8 cm^3 mol^{-1}), $[Ru(OH_2)_6]^{2+}$ (−0.4 cm^3 mol^{-1}); $[Fe(OH_2)_6]^{3+}$ (−5.4 cm^3 mol^{-1}), $[Ru(OH_2)_6]^{3+}$ (−8.3 cm^3 mol^{-1}); $[Rh(OH_2)_6]^{3+}$ (−4.2 cm^3 mol^{-1}), $[Ir(OH_2)_6]^{3+}$ (−5.7 cm^3 mol^{-1})].[2−6] This increasingly associative character is explained as resulting from a gradual increase in ionic radii, which allows for more association with the incoming ligand.[14,15] These trends led us to wonder if they persist for larger multinuclear clusters. The ideal

* To whom correspondence should be addressed. E-mail: whcasey@ucdavis.edu.
[†] Department of Chemistry, University of California, Davis.
[§] Department of Geology, University of California, Davis.
[‡] University of St. Andrews.

(1) Merbach, A. E.; Vanni, H. *Helv. Chim. Acta* **1977**, *60*, 1124−7.
(2) Ducommun, Y.; Newman, K. E.; Merbach, A. E. *Inorg. Chem.* **1980**, *19*, 3696−703.
(3) Rapaport, I.; Helm, L.; Merbach, A. E.; Bernhard, P.; Ludi, A. *Inorg. Chem.* **1988**, *27*, 873−9.
(4) Swaddle, T. W.; Merbach, A. E. *Inorg. Chem.* **1981**, *20*, 4212−16.
(5) Laurenczy, G.; Rapaport, I.; Zbinden, D.; Merbach, A. E. *Magn. Reson. Chem.* **1991**, *29* (Special Issue), S45−S51.
(6) Cusanelli, A.; Frey, U.; Richens, D. T.; Merbach, A. E. *J. Am. Chem. Soc.* **1996**, *118*, 5265−5271.
(7) Pittet, P.-A.; Elbaze, G.; Helm, L.; Merbach, A. E. *Inorg. Chem.* **1990**, *29*, 1936−42.
(8) Bleuzen, A.; Pittet, P.-A.; Helm, L.; Merbach, A. E. *Magn. Reson. Chem.* **1997**, *35*, 765−773.
(9) Sisley, M. J.; Yano, Y.; Swaddle, T. W. *Inorg. Chem.* **1982**, *21*, 1141−5.
(10) Swaddle, T. W. *Inorg. Chem.* **1980**, *19*, 3203−5.
(11) Tong, S. B.; Krouse, H. R.; Swaddle, T. W. *Inorg. Chem.* **1976**, *15*, 2643−4.
(12) Weekes, M. C.; Swaddle, T. W. *Can. J. Chem.* **1975**, *53*, 3697−701.
(13) Guastalla, G.; Swaddle, T. W. *Can. J. Chem.* **1973**, *51*, 821−7.
(14) Merbach, A.E; Akitt, J. W. *High-resolution variable pressure NMR for chemical kinetics, NMR Basic Principles and Progress*; Springer-Verlag: Berlin; Heidelberg, 1990; Vol. 24, p 201.
(15) Helm, L.; Merbach, A. E. *Chem. Rev.* **2005**, *105*, 1923−1959.

10.1021/ic0609608 CCC: $33.50 © 2006 American Chemical Society
Published on Web 08/25/2006

experimental test would involve molecules containing isoelectronic metal ions located within the same group.

Only recently have researchers begun to conduct high-pressure ^{17}O NMR experiments on aqueous multinuclear clusters and hydrolytic oligomers.[16−18] To our knowledge, there are only three such high-pressure ^{17}O NMR studies on clusters (see also Murmann and Giese, 1978[19]). The high-pressure ^{17}O NMR study on the polyoxocation $GaO_4Al_{12}(OH)_{24}(H_2O)_{12}^{7+}$ (**GaAl**$_{12}$) was the first of its kind because not only was an activation volume for water exchange reported ($\Delta V^{\ddagger} = +3$ cm^3 mol^{-1}) but also for exchange of one of the hydroxyl-bridge sites ($\Delta V^{\ddagger} = +7$ cm^3 mol^{-1}).[16] Houston et al. (2005) recently reported the pressure dependence of water exchange from the acetate-bridged oxo-centered rhodium(III) trimer, $[Rh_3(\mu_3\text{-}O)(\mu\text{-}O_2CCH_3)_6(OH_2)_3]^+$ (abbreviated as **Rh**$_3^+$) and found that the activation pathway followed an dissociative-interchange mechanism ($\Delta V^{\ddagger} = +5.3$ cm^3 mol^{-1}).[17] This positive activation volume contrasts with the negative value (−4.2 cm^3 mol^{-1})[5] for water exchange on octahedral monomeric $[Rh(OH_2)_6]^{3+}$ and is attributed to labilization from the planar μ_3-oxo, facilitating a more dissociative water-exchange mechanism for this trinuclear cluster. Activation volumes for exchange of the cis and trans water molecules from the hydroxo-bridged rhodium(III) dimer (abbreviated as **Rh**$_2^{4+}$) also indicate highly dissociative activation pathways [$\Delta V^{\ddagger} = +8.5$ cm^3 mol^{-1} (*trans*); +10.1 cm^3 mol^{-1} (cis)],[18] which contrasts with the behavior of monomeric $[Rh(OH_2)_6]^{3+}$. One should bear in mind, however, that the extent to which Swaddle's interpretations of activation volumes, which were established for octahedral monomeric ions of the 3d series (Associative (A) = $\Delta V^{\ddagger} \approx -13$; Interchange (I) = $\Delta V^{\ddagger} \approx 0$; or Dissociative (D) = $\Delta V^{\ddagger} \approx +13$),[20] can be extended to large clusters is yet to be fully established.

To extend the field, we have chosen to examine water exchange from the bioxo-capped M−M-bonded trinuclear clusters, $[M_3(\mu_3\text{-}O)_2(\mu\text{-}O_2CCH_3)_6(OH_2)_3]^{2+}$ (M = Mo(IV) and W(IV)) [abbreviated in subsequent text as **Mo**$_3^{2+}$ and **W**$_3^{2+}$]. These clusters are particularly good candidates for study because previous water-exchange experiments exhibited markedly different activation parameters (**Mo**$_3^{2+}$: $\Delta H^{\ddagger} = 126$ kJ mol^{-1}, $\Delta S^{\ddagger} = 77$ J mol^{-1} K^{-1}; **W**$_3^{2+}$: $\Delta H^{\ddagger} = 58$ kJ mol^{-1}, $\Delta S^{\ddagger} = -164$ J mol^{-1} K^{-1}),[21] indicating a unique changeover in the exchange mechanism even though these two clusters possess very similar, almost identical, structures. Thus, these two clusters afford the rare opportunity to investigate how the tetravalent transition metal ion alone influences the water-exchange mechanism.

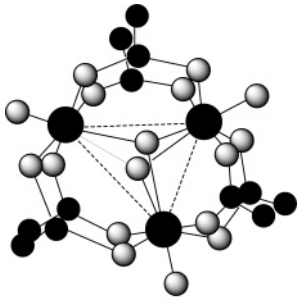

$[M_3(\mu_3\text{-}O)_2(\mu\text{-}O_2CCH_3)_6(OH_2)_3]^{2+}$
(M = Mo(IV) and W(IV))

[abbreviated as **Mo**$_3^{2+}$ and **W**$_3^{2+}$]

Materials and Methods

Solutions. Perchlorate salts of the metal complexes were prepared using the method of Powell et al.[21] Characterization of the powder was performed using UV−vis (**Mo**$_3^{2+}$, $\lambda_{max} = 509$ nm, $\lambda = 430$ nm; **W**$_3^{2+}$ $\lambda_{max} = 444$ nm, $\lambda = 358$ nm)[21] and ^1H NMR (δ **Mo**$_3^{2+}$(μ-O_2CCH_3) = 2.31 ppm; δ **W**$_3^{2+}$(μ-O_2CCH_3) = 2.39 ppm; CD_3OD, $T = 298$ K) to ensure the purity of the compounds prior to performing the exchange experiments.

For the ^{17}O NMR kinetic experiments, the appropriate amount of the **Mo**$_3^{2+}$ perchlorate salt was dissolved in 2.4 mL of $^{17}OH_2$ (40%) to give a cluster concentration of 10 mM. To observe the bound water (η-OH_2) signal at +94 ppm, the large bulk water signal was broadened beyond detection by the addition of $[Mn(OH_2)_6](ClO_4)_2$ to give a $[Mn^{2+}] = 0.1$ M.[22] All solutions were acidified with $HClO_4$ ($[H^+] = 0.6$ M) to ensure that the complexes were in their fully protonated forms[21] and augmented with $NaClO_4$ to give $I = 1.0$ M. Perchlorate was chosen because it provides a signal downfield (301 ppm; $T = 298$ K) that can be used as a constant-intensity internal standard. After the solutions were mixed, the samples were subsequently filtered through a 0.22 μm filter to remove any suspended particulates. To prevent oxidation at the experimental temperature ($T = 310.3$ K), samples were flushed with argon for 10−15 min. After the kinetic experiments were complete, UV−vis spectra were collected on all samples in order to ensure that no degradation or polymerization had occurred during the measurements.

Because **W**$_3^{2+}$ is prone to oxidation in high perchlorate concentrations, samples were prepared using CF_3SO_3H/CF_3SO_3Na according to the method of Powell et al.[21] Other than this difference in background electrolyte, the sample preparation and reagent concentrations were nearly identical to those used for **Mo**$_3^{2+}$; [**W**$_3^{2+}$] = 10 mM, $[H^+] = 0.6$ M. To see the η-OH_2 signal at +83 ppm, $[Mn(OH_2)_6](CF_3SO_3)_2$ was added to give a $[Mn^{2+}] = 0.1$ M. Since there was insufficient perchlorate to provide an internal standard for the rate measurements, 50 μL of $Al(OH_2)_6^{3+}$ (prepared from the perchlorate salt, $[Al^{3+}] = 250$ mM) was added to the solution. This signal (+28 ppm) provided a stable and constant reference throughout the experiment because the η-OH_2 on the Al^{3+} ion are in isotopic-exchange equilibrium with the bulk water at the experimental temperature ($T = 333.3$ K). Because the temperature was relatively high and the solution extremely acidic ($[H^+] = 0.6$ M), no hydrolysis products from Al^{3+} were detected on the ^{17}O NMR spectrum.

Variable-Pressure ^{17}O NMR Spectroscopy. ^{17}O NMR spectra were acquired in unlocked mode on a Bruker AQS500 NMR

(16) Loring, J. S.; Yu, P.; Phillips, B. L.; Casey, W. H. *Geochim. Cosmochim. Acta* **2003**, *68*, 2791−2798.
(17) Houston, J. R.; Yu, P.; Casey, W. H. *Inorg. Chem.* **2005**, *44*, 5176−5182.
(18) Drljaca, A.; Zahl, A.; Van Eldik, R. *Inorg. Chem.* **1998**, *37*, 3948−3953.
(19) Murmann, R. K.; Giese, K. C. *Inorg. Chem.* **1978**, *17*, 1160−1166.
(20) Swaddle, T. W. *Inorg. Chem.* **1983**, *22*, 2663−5.
(21) Powell, G.; Richens, D. T. *Inorg. Chem.* **1993**, *32*, 4021−9.
(22) Swift, T. J.; Connick, R. E. *J. Chem. Phys.* **1962**, *37*, 307−320.

spectrometer equipped with a wide-bore (89 mm) 11.7 T magnet located at the University of California, Davis, Keck Nuclear Magnetic Resonance Facility. Spectral data was collected at $\nu_0 =$ 67.8 MHz with single-pulse excitation using a pulse length of 30 μs ($\pi/2 = 60$ μs), a sweep width of 95 kHz, and a recycle delay of 15 ms. Averaging of 55 000 scans for $\mathbf{Mo}_3^{2+}$ and 120 000 for $\mathbf{W}_3^{2+}$ was used to achieve adequate signal-to-noise. To ensure the B_0 field was homogeneous, the magnet was shimmed on a 0.1 M Al^{3+} solution in an identical high-pressure tube at all experimental pressures and temperatures (^{27}Al line-width 5−7 Hz; ^{17}O line-width 100−150 Hz, depending on temperature). To remove baseline roll due to acoustic ringing, the first 12 data points were recalculated from the remainder of the free-induction decay using a backward linear-prediction algorithm. All chemical shifts are referenced to an external source of tap water (0 ppm; coaxial insert; $T = 298$ K); however, all samples contained paramagnetic Mn^{2+}, and so ^{17}O signals may be slightly shifted relative to previously published data.[21]

All ^{17}O NMR measurements were made using a high-pressure NMR probe assembly (titanium alloy vessel: 61.5 mm o.d., 20 mm i.d.; pressurizing fluid: *n*-hexanes), which has been described in detail elsewhere.[16,17,23] To transmit pressure to the sample, the solution was placed inside a quartz NMR tube (two 8 mm o.d. tubes connected via a capillary) and sealed with a movable PTFE piston seated with two O-rings.[23] The movable piston allows pressure from the *n*-hexanes to be transferred to the sample from the pressure-generating system (a large-volume manual syringe pump; High-Pressure Research, Inc.).

Data were acquired at $P = 6$, 52, 102, 150, 202, and 250 MPa ($T = 310.3$ K) for $\mathbf{Mo}_3^{2+}$ and $P = 10$, 60, 110, 176, and 229 MPa ($T = 333.3$ K) for $\mathbf{W}_3^{2+}$. By circulating water through the probe jacket, the sample temperature was controlled to within ±0.2 K. Temperature was continuously monitored with a copper−constantan thermocouple symmetrically disposed from the sample inside the pressure chamber. Experimental pressures were also measured continuously with an electronic gauge (High-Pressure Research, Inc.) and controlled to within ±4 MPa or better. Before data acquisition commenced, the solutions were allowed to thermally equilibrate for 60 min at the experimental temperatures and pressures.

Kinetic Analysis. Rates of water exchange were determined by monitoring the height of the ^{17}O NMR signal from the η-OH_2 as a function of time. To account for any instrumental fluctuations during the kinetic run, peak heights were normalized to an internal standard, which was the ClO_4^- signal for $\mathbf{Mo}_3^{2+}$ and η-OH_2 on the Al^{3+} ion for $\mathbf{W}_3^{2+}$. All ^{17}O NMR signals were fit to Lorentzian curves. To calculate a pseudo-first-order rate coefficient, the normalized peak heights were fit to a standard three-parameter exponential growth equation (eq 1).[17]

$$I_t = I_0 + a(1 - e^{-k_{ex}t}) \tag{1}$$

The term k_{ex} refers to the rate coefficient for water exchange, a is an adjustable parameter, and t is the elapsed time after mixing. The term I_0 is the normalized height of the bound water resonance at $t = 0$, which was chosen as an adjustable parameter because it took nearly an hour for the sample to equilibrate to temperature. The term I_t refers to the normalized peak height during the course of the experiment.

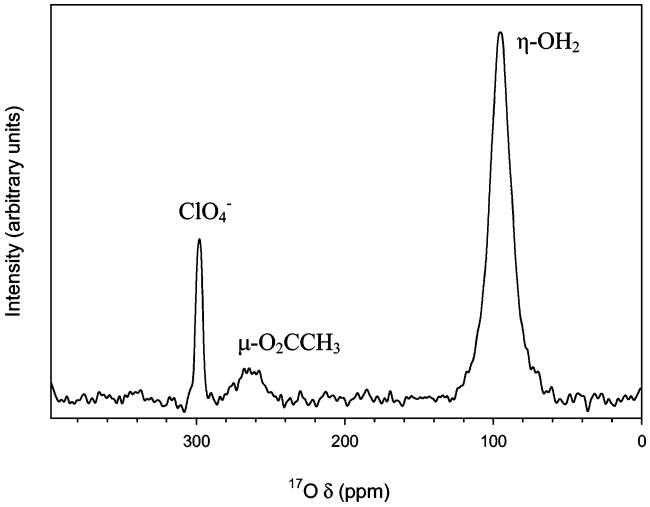

Figure 1. ^{17}O NMR spectrum for $\mathbf{Mo}_3^{2+}$ at $T = 310.3$ K and $P = 250$ MPa; $[\mathbf{Mo}_3^{2+}] = 10$ mM, $[Mn^{2+}] = 0.1$ M, $[H^+] = 0.6$ M, $I = 1.0$ M($NaClO_4$). Signals at +94 and ∼263 ppm are from η-OH_2 and μ-O_2-CCH_3, respectively. This spectrum was collected following equilibration of η-OH_2 sites using 55 000 scans at $\nu_0 = 67.8$ MHz with single-pulse excitation of 30 μs, 15 ms pulse delay, and a sweep width of 95 kHz.

The variation of reaction rate with pressure can be related to the activation volume ($\Delta V^{\ddagger}$) by eq 2.[24]

$$\left(\frac{\partial \ln(k_{ex})}{\partial P}\right)_T = -\frac{\Delta V^{\ddagger}}{RT} \tag{2}$$

The terms P and T are the experimental pressure and temperature, respectively. Assuming that the compressibility of the molecules is negligible over the pressure range studied here (6−250 MPa), eq 3 applies and allows the direct calculation of $\Delta V^{\ddagger}$.[24−26]

$$\ln(k_{ex,P}) = \ln(k_{ex,P=0}) - \frac{P\Delta V^{\ddagger}}{RT} \tag{3}$$

The terms $k_{ex,P}$ and $k_{ex,P=0}$, refer to the rate constant at the experimental pressure and at zero pressure, respectively. For water-exchange reactions in which there is no creation or destruction of charge, electrostriction effects can safely be ignored. Therefore, $\Delta V^{\ddagger}$ can be directly diagnostic of geometrical changes, such as bond-breaking and making during the formation of the activated complex.[24−26]

Results

^{17}O NMR Spectra. A typical ^{17}O NMR spectrum for $\mathbf{Mo}_3^{2+}$ is shown in Figure 1. This spectrum, as well as the ^{17}O NMR spectrum for the $\mathbf{W}_3^{2+}$ trimer [$\delta(\eta$-$OH_2) = +83$ ppm; ∼1 kHz; not shown], shows a broad signal for the η-OH_2 (+94 ppm), ∼1 kHz wide. When compared to $\mathbf{Rh}_3^{+}$, these line widths are greater by nearly 800 Hz [$\delta(\eta$-$OH_2) = -57$ ppm; ∼285 Hz at $T = 298$K].[17] Because magnetic-susceptibility measurements for $\mathbf{Mo}_3^{2+}$ indicate that this trinuclear structure is diamagnetic,[27] lower symmetry at the M-OH_2 sites is most likely responsible for the significant line-broadening effect via rapid quadrupolar relaxation. Also

(23) Jonas, J.; Koziol, P.; Peng, X.; Reiner, C.; Campbell, D. *J. Magn. Reson. B* **1993**, *102*, 299.
(24) Merbach, A. E. *Pure Appl. Chem.* **1982**, *54*, 1479.
(25) Richens, D. T. *The Chemistry of Aqua Ions*; John-Wiley: Chichester; New York, 1997.
(26) Wilkins, R. G. *Kinetics and Mechanism of Reactions of Transition Metal Complexes*, 2nd ed.; VCH: Weinheim, Germany, 1991.
(27) Bino, A.; Cotton, F. A.; Dori Z. *J. Am. Chem. Soc.* **1981**, *103*, 243−244.

Table 1. Kinetic Data for Water Exchange from $[M_3(\mu_3\text{-}O)_2(\mu\text{-}O_2CCH_3)_6(OH_2)_3]^{2+}$ (M = Mo(IV) and W(IV))

complex	temp (K)	pressure (MPa)	$10^5\ k_{ex}\ (s^{-1})$
Mo(IV)	310.3	6 (±3)	3.13 (±0.26)
		52 (±3)	2.61 (±0.11)
		102 (±3)	2.37 (±0.22)
		150 (±4)	2.01 (±0.12)
		202 (±3)	1.65 (±0.28)
		250 (±4)	1.47 (±0.08)
W(IV)	333.3	10 (±1)	0.583 (±0.020)
		60 (±2)	0.601 (±0.020)
		110 (±2)	0.618 (±0.017)
		176 (±2)	0.655 (±0.024)
		229 (±3)	0.681 (±0.017)

shown on the $\mathbf{Mo_3}^{2+}$ spectrum is a broad signal at ~263 ppm [$\mathbf{W_3}^{2+}$; $\delta(\mu\text{-}O_2CCH_3)$ = ~247 ppm] assigned to spin-labeled ^{17}O in the acetate bridges ($\mu\text{-}O_2CCH_3$), which was observed for $\mathbf{Rh_3}^{+}$ ($\delta(\mu\text{-}O_2CCH_3)$ = 131 ppm) as well.[17] Kinetic data for more than one half-life could not be obtained within a reasonable period of time due to the slow exchange rates at the experimental temperatures. Isotopic substitution into the capping oxos (μ_3-O) was not observed.

Variable-Pressure Kinetics. Over the course of the exchange experiment, the peak height of the isotopically tagged η-OH_2 grew exponentially as a function of time. Peak heights were normalized to a constant-intensity internal standard (see Materials and Methods) and plotted versus time to extract pseudo-first-order rate coefficients using eq 1. For $\mathbf{Mo_3}^{2+}$, this experiment was repeated at six pressures (P = 6, 52, 102, 150, 202, and 250 MPa; T = 310.3 K), and for $\mathbf{W_3}^{2+}$, the exchange experiment was repeated at five pressures (P = 10, 60, 110, 176, and 229 MPa; T = 333.3 K) (Table 1). Water-exchange data indicate that, with increasing pressure, the rate constants decrease by a factor of 2 for $\mathbf{Mo_3}^{2+}$ (P = 6−250 MPa) and increase by a factor of 1.2 (P = 10−229 MPa) for $\mathbf{W_3}^{2+}$. Selected kinetic data for both $\mathbf{Mo_3}^{2+}$ and $\mathbf{W_3}^{2+}$experiments are shown in Figure 2 ($\mathbf{Mo_3}^{2+}$, first 33 h; $\mathbf{W_3}^{2+}$, first 97 h) to illustrate the pressure dependence of the reaction rates. To calculate a reliable rate constant, exchange experiments for the $\mathbf{Mo_3}^{2+}$ were typically monitored for 2.5 days and for the more inert $\mathbf{W_3}^{2+}$, experiments were monitored for 5−6 days.

A plot of $\ln[k_{ex}\ (s^{-1})]$ vs pressure (atm) allows for the calculation of $\Delta V^{\ddagger}$ from a weighted least-squares fit of the line (eq 3). Volumes of activation were calculated as $\Delta V^{\ddagger}$ = +8.0 (±0.4) $cm^3\ mol^{-1}$ for $\mathbf{Mo_3}^{2+}$ and $\Delta V^{\ddagger}$ = −1.9 (±0.2) $cm^3\ mol^{-1}$ for $\mathbf{W_3}^{2+}$. Shown in Figure 3 are the pressure-dependent kinetic data for the $\mathbf{Mo_3}^{2+}$ and $\mathbf{W_3}^{2+}$ experiments, in addition to the previously published data for $\mathbf{Rh_3}^{+}$ [$\Delta V^{\ddagger}$ = +5.3 (±0.4) $cm^3\ mol^{-1}$].[17]

Discussion

Although these two molecules are nearly isostructural (M−OH_2 = 2.129, 2.128 Å; M−M = 2.759, 2.747 Å; M−μ_3-O = 1.994−2.000 Å; M = Mo(IV),W(IV), CF_3SO_3 salts)[28,29] and have similar exchange rates ($k_{ex}^{298}(\mathbf{Mo_3}^{2+})$ = 5.6 × 10^{-6} s^{-1} and $k_{ex}^{298}(\mathbf{W_3}^{2+})$ = 1.0 × 10^{-6} s^{-1}),[21] the activation volumes are strikingly different ($\mathbf{Mo_3}^{2+}$: +8.0 $cm^3\ mol^{-1}$; $\mathbf{W_3}^{2+}$: −1.9 $cm^3\ mol^{-1}$). Although Swaddle's model for assigning mechanisms from activation volumes[10] is not yet

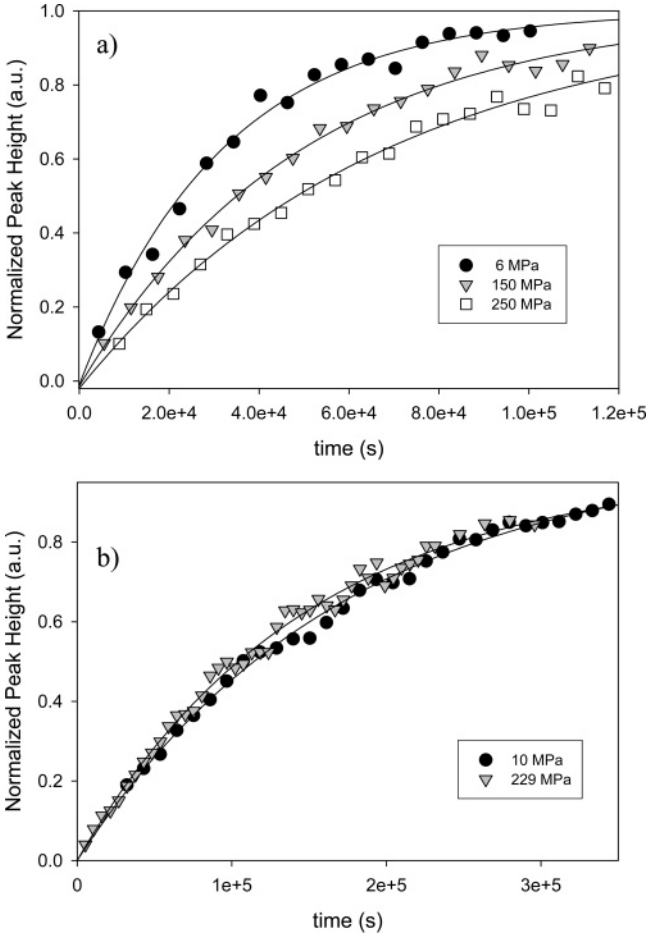

Figure 2. Variation of the normalized intensity of the η-OH_2 signal as a function of time. Lines are weighted least-squares fits to eq 1. For $\mathbf{Mo_3}^{2+}$, water-exchange rates decrease with increasing pressure (6, 150, 250 MPa) (a) and for $\mathbf{W_3}^{2+}$, reaction rates increase with increasing pressure (10 and 229 MPa) (b).

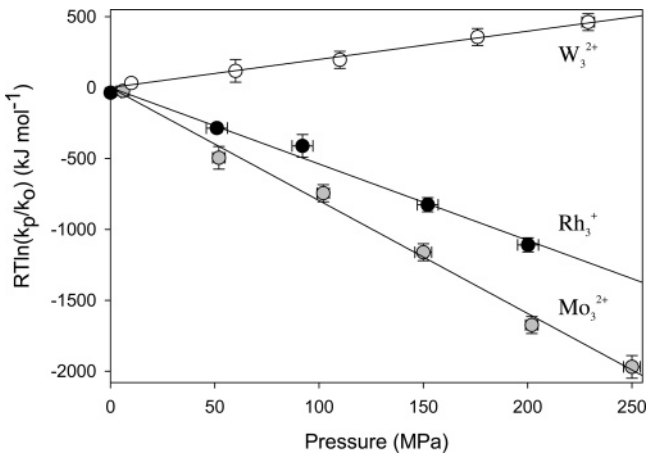

Figure 3. Pressure dependence of the pseudo-first-order rate coefficient for water exchange from $\mathbf{Mo_3}^{2+}$ (gray circle), $\mathbf{W_3}^{2+}$ (empty circle), and $\mathbf{Rh_3}^{+}$ (black circle) clusters. The lines correspond to a weighted least-squares fit to eq 3, which yields $\Delta V^{\ddagger}$ = +8.0 (±0.4) $cm^3\ mol^{-1}$ for $\mathbf{Mo_3}^{2+}$ and $\Delta V^{\ddagger}$ = −1.9 (±0.2) $cm^3\ mol^{-1}$ for $\mathbf{W_3}^{2+}$. The data for $\mathbf{Rh_3}^{+}$ are from ref 17 ($\Delta V^{\ddagger}$ = +5.3 (±0.4) $cm^3\ mol^{-1}$).

(28) Cotton, F. A.; Dori, Z.; Marler, D. O.; Schwotzer, W. *Inorg. Chem.* **1983**, *22*, 3104−3106.
(29) Bino, A.; Cotton, F. A.; Dori, Z.; Koch, S.; Kuppers H.; Millar, M.; Sekutowski, J. C. *Inorg. Chem.* **1978**, *17*, 3245−3253.

verified for multinuclear molecules such as these, the new experimental data clearly indicate a change in mechanism. Using his semiempirical model [Associative (A) = $\Delta V^{\ddagger} \approx -13$; Interchange (I) = $\Delta V^{\ddagger} \approx 0$; or Dissociative (D) = $\Delta V^{\ddagger} \approx +13$], the water exchange mechanism changes from D or I_d ($\mathbf{Mo_3}^{2+}$) to I_a ($\mathbf{W_3}^{2+}$), which is consistent with other distinctly different activation parameters, [$\mathbf{Mo_3}^{2+}$: $\Delta H^{\ddagger} = 126$ kJ mol^{-1}, $\Delta S^{\ddagger} = 77$ J mol^{-1} K^{-1}; and for $\mathbf{W_3}^{2+}$: $\Delta H^{\ddagger} = 58$ kJ mol^{-1}, $\Delta S^{\ddagger} = -164$ J mol^{-1} K^{-1}].[21] These volumes represent the largest difference in $\Delta V^{\ddagger}$ values ($\sim$10 cm^3 mol^{-1}) for any two isostructural 4d−5d and 3d−4d metal species located within the same group, and based on their different magnitudes, demonstrate a unique mechanistic changeover.[30] These data may become as useful as the changeover in mechanism for octahedral first row transition metal ions that has served as a reliable test case for computer simulations.[31,32]

For isoelectronic metal ions with the same coordination geometry, as is the case for $\mathbf{Mo_3}^{2+}$ and $\mathbf{W_3}^{2+}$, the size of the metal ion dictates the activation pathway. Large ions typically have more room for association with the entering molecule.[15] Unfortunately, however, Mo(IV) and W(IV) ionic radii for nonacoordination, as in these trimeric molecules, are not available to compare. We anticipate that ionic radii for the nine-coordinate Mo(IV) and W(IV) would be similar to one another because of the lanthanide contraction. For example, these metals in hexacoordination have ionic radii of 65 and 66 pm, respectively, for Mo(IV) and W(IV).[33] The local structures around each of the metal ions are also similar and do not immediately suggest a reason that one pathway would be considerably more dissociative than the other. For example, the angle between μ-O_2CCH_3 and the η-OH_2 [e.g., $(CH_3CO)O-M-O(OH_2)$] for both molecules is roughly 75°,[28,34] as estimated from crystal data. Although crowding around the metal center would inhibit attack by the incoming ligand and lead to a more dissociative activation state, we only see evidence for a dissociative pathway for the $\mathbf{Mo_3}^{2+}$ cluster, yet crowding is similar in the $\mathbf{W_3}^{2+}$ molecule.

The profound difference in mechanism for these otherwise similar molecules suggests that they might be well suited for simulation,[31,32,35] which we have underway. Preliminary data from DFT calculations (B3LYP/LANL2DZ)[36] indicate a difference in bonding character from the metal centers to the ligands for the $\mathbf{Mo_3}^{2+}$ and $\mathbf{W_3}^{2+}$ clusters in their ground states. The NBO charges at the tetravalent metal are significantly different for the two clusters; the NBO charge on W(IV) is slightly greater than Mo(IV) [Mo(IV) = +1.424; W(IV) = +1.698]. Correspondingly, the oxygen atoms in the coordinated ligands have greater negative NBO charge in $\mathbf{W_3}^{2+}$ versus $\mathbf{Mo_3}^{2+}$ [$\mathbf{Mo_3}^{2+}$: $H_3CCOO = -0.672/-0.640$, $H_2O = -0.871$; $\mathbf{W_3}^{2+}$: $H_3CCOO = -0.677/-0.713$, $H_2O = -0.899$). These data indicate a larger degree of charge separation in the $\mathbf{W_3}^{2+}$ cluster and thus greater bond polarity. We speculate that this greater charge separation stabilizes the incoming water molecule during the formation of the transition-state complex, resulting in a more associatively activated pathway for $\mathbf{W_3}^{2+}$. A comprehensive and detailed computational study aimed to simulate the activation barrier for both molecules is currently underway.

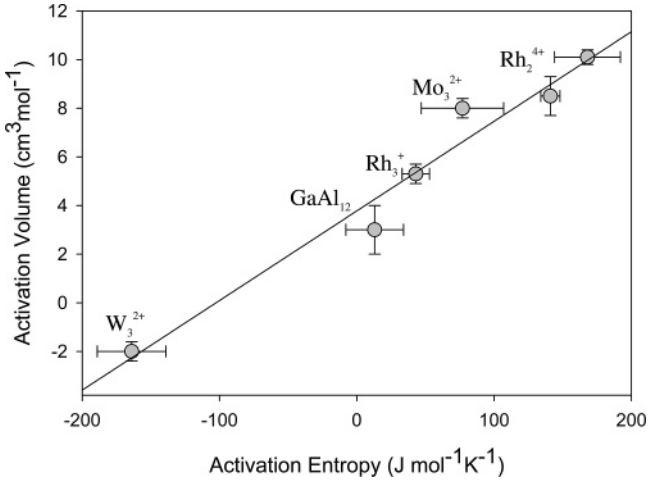

Figure 4. Volumes of activation and entropies for water exchange from multinuclear metal complexes. The data presented above are from this work and refs 16−18. Two points are plotted for the $\mathbf{Rh_2}^{4+}$ cluster corresponding to separate rates for the bound waters that are cis and trans to the μ_2-OH bridge.

The reactivity trends that we observe here for the trinuclear clusters are qualitatively consistent with trends evident in the 4d−5d group monomeric aqua ions. Exchange mechanisms for monomeric ions become increasingly associative deeper in the 4d−5d group.[15] For example, water exchange becomes more associative for the larger $Ir(OH_2)_6^{3+}$ vs the slightly smaller $Rh(OH_2)_6^{3+}$ ion (Rh(III) = 0.665 Å, Ir(III) = 0.680 Å)[33] based on the reported activation volumes ($\Delta V^{\ddagger} = -4.2$ and -5.7 cm^3 mol^{-1}, respectively).[5,6] As another example, albeit not for octahedral ions, the activation volume for $[Pt(OH_2)_4]^{2+}$ ($\Delta V^{\ddagger} = -4.6$ cm^3 mol^{-1}) is more negative than that of $[Pd(OH_2)_4]^{2+}$ ($\Delta V^{\ddagger} = -2.2$ cm^3 mol^{-1}),[37,38] even though the ionic radius of Pt(II) is smaller (Pd(II) = 0.64 Å, Pt(II) = 0.60 Å).[33] These examples demonstrate an increase in associative character as one goes deeper into the group, but not a drastic change in mechanism, such as we find here for the trinuclear clusters.

Most importantly, there are now enough high-pressure ^{17}O NMR data to establish mechanistic trends for several multinuclear aqueous complexes. The data compiled in Figure 4 show that activation volumes for water exchange correlate linearly with the corresponding activation entropies. Similar trends have been previously found for water ex-

(30) Helm, L.; Merbach, A. E. *J. Chem. Soc., Dalton Trans.* **2002**, *5*, 633−641.
(31) Rotzinger, F. P. *Helv. Chim. Acta* **2000**, 83, 3006−3020.
(32) Rotzinger, F.P. *J. Am. Chem. Soc.* **1997**, *119*, 5230−5238.
(33) Shannon, R. D. *Acta Crystallogr., Sect. A* **1976**, *32*, 751−767.
(34) Bino, A.; Hesse, K. F.; Kueppers, H. *Acta Crystallogr., Sect. B* **1980**, *B36*, 723−725.
(35) (a) Stack, A. G.; Rustad, J. R.; Casey, W.H *J. Phys. Chem. B* **2005**, 109, 23771−23775. (b) Rotzinger, F. P. *Chem. Rev.* **2005**, 105, 2003−2037.
(36) Glendening, E. D.; Weinhold, F. *J. Comp. Chem.* **1998**, *19*, 610−627.
(37) Helm, L.; Elding L. I.; Merbach, A. E. *Helv. Chim. Acta* **1984**, *67*, 1453−60.
(38) Helm, L.; Elding L. I.; Merbach A. E. *Inorg. Chem.* **1985**, *24*, 1719−21.

change and racemization at monomeric metal ions (see Twigg (1977) and Wilkins (1991)),[26,39] but not for molecular clusters such as those we present here. This correlation includes reactions with profoundly different mechanisms (D to I_a) and for a variety of aqueous clusters with vastly different molecular structures (e.g., $\mathbf{GaAl_{12}}$ vs $\mathbf{Mo_3^{2+}}$). One extreme is provided by the recent study of solvent exchange on the $\mathbf{Rh_2^{4+}}$ ion by Drljaca et al.,[18] who report $\Delta V^{\ddagger}$ for the cis and trans waters of the rhodium(III) dimer to be +8.5 (±0.8) and +10.1 (±0.8) $cm^3\ mol^{-1}$, both of which correspond to a D mechanism. These are the largest values yet measured for clusters and serve as the upper limit in Figure 4, although the $\Delta V^{\ddagger}$ values are smaller than the +13 $cm^3\ mol^{-1}$ originally suggested by Swaddle for simple octahedral metal ions. Recently though, $\Delta V^{\ddagger}$ values of ~+9 $cm^3\ mol^{-1}$ have been assigned to the limiting D pathway.[40,41] The rationale for this reassignment is that the effective radius of a water molecule is reduced in a close-packed structure. Expulsion of a bound water from this close-packed structure to the bulk would result in a volume change of ~18−9 = ~+9 $cm^3\ mol^{-1}$. The datum that we report here for the $\mathbf{W_3^{2+}}$ molecule provides the other limiting extreme in the experimental measurements. The extent to which this molecule exchanges water via a purely A or I_a pathway is not yet established, although we suspect that it is clearly more associative than the activation volume indicates.

Predictions fall directly from the correlation in Figure 4. For example, rate parameters for the mono-oxo-capped mixed-valence W(III,III,IV) trimer are also consistent with a similar associative activation pathway for water exchange ($\Delta H^{\ddagger}$ = 53 kJ mol^{-1}, $\Delta S^{\ddagger} = -131\ Jmol^{-1}K^{-1}$).[21] Using the correlation in Figure 4, we predict that the $\Delta V^{\ddagger}$ value should fall near the $\mathbf{W_3^{2+}}$ ion of slightly less than 0 $cm^3\ mol^{-1}$, for which we await experimental verification. This type of correlation could turn out to be an extremely powerful tool for predicting mechanisms of ligand exchange for a variety of molecular clusters on the basis of the activation entropies alone. We do recognize, however, that activation entropies can carry large experimental uncertainties due to extrapolation to infinite temperature. In addition, factors that remain to be evaluated include the compressibility of the molecules, which might differ considerably from monomeric species, and the extent to which the transmission coefficients vary with pressure. Both of these uncertainties, however, can be assessed by computation. Even without the simulations, however, the high-pressure ^{17}O NMR data allow us to establish key reactivity trends and show that the values of $\Delta V^{\ddagger}$ are not vastly different than what is expected from the many studies of aqueous monomer complexes.[15]

(39) Twigg, M. V. *Inorg. Chim. Acta* **1977**, *24*, L84-L86.
(40) Richens, D. T. *Chem. Rev.* **2005**, *105*, 1961−2002.
(41) Richens, D. T. *Comm. Inorg. Chem.* **2005**, *26*, 217−232.

Conclusions

Mechanisms for water exchange from the bioxo-capped M−M-bonded trinuclear clusters, $[M_3(\mu_3\text{-}O)_2(\mu\text{-}O_2CCH_3)_6(OH_2)_3]^{2+}$ (M = Mo(IV) and W(IV)) are profoundly different, although the clusters are virtually isostructural. The difference in activation volume is the largest (~10 $cm^3\ mol^{-1}$) yet reported for any 4d−5d (and 3d−4d) isostructural transition metal ions located in the same group of the periodic table. These volumes, when combined with high-pressure ^{17}O NMR data from other aqueous metal clusters, allow us to establish a strong correlation between the activation volumes and entropies. This correlation can be used to assign mechanisms for water-exchange reactions for a variety of different aqueous metal clusters.

Acknowledgment. The authors gratefully acknowledge Prof. James Rustad for helpful discussions on the simulation results. We also thank three anonymous referees for their comments and suggestions. Support for this research was from ACS (PRF Grant No. 40412-AC2). We acknowledge the Keck Foundation for support of the solid-state NMR center at UC Davis.

IC0609608